

Article

Synthesis, Thermal Behavior, and Mechanical Properties of Fully Biobased Poly(Hexamethylene 2,5-Furandicarboxylate-Co-Sebacate) Copolyesters

Shiwei Feng, Zhiguo Jiang * and Zhaobin Qiu * 

State Key Laboratory of Chemical Resource Engineering, Beijing University of Chemical Technology, Beijing 100029, China

* Correspondence: jiangzg@mail.buct.edu.cn (Z.J.); qiuzb@mail.buct.edu.cn (Z.Q.)

Abstract: In this research, three fully biobased poly(hexamethylene 2,5-furandicarboxylate-co-sebacate) (PHFSe) copolyesters with low contents of hexamethylene sebacate (HSe) unit (10 mol%, 20 mol%, and 30 mol%) were successfully synthesized through a two-step transesterification/esterification and polycondensation method. The chemical structure and actual composition of PHFSe copolyesters were confirmed by hydrogen nuclear magnetic resonance. The thermal behavior and mechanical property of PHFSe copolyesters were investigated and compared with those of the poly(hexamethylene 2,5-furandicarboxylate) (PHF) homopolymer. Both PHFSe copolyesters and PHF showed the high thermal stability. The basic thermal parameters, including glass transition temperature, melting temperature, and equilibrium melting temperature, gradually decreased with increasing the HSe unit content. PHFSe copolyesters crystallized more slowly than PHF under both the nonisothermal and isothermal melt crystallization conditions; however, they crystallized through the same crystallization mechanism and crystal structure. In addition, the mechanical property, especially the elongation at break of PHFSe copolyesters, was obviously improved when the HSe unit content was greater than 10 mol%. In brief, the thermal and mechanical properties of PHF may be easily tuned by changing the HSe unit content to meet various practical end-use requirements.

Keywords: biobased; crystallization; mechanical property; structure and property relationship



Citation: Feng, S.; Jiang, Z.; Qiu, Z. Synthesis, Thermal Behavior, and Mechanical Properties of Fully Biobased Poly(Hexamethylene 2,5-Furandicarboxylate-Co-Sebacate) Copolyesters. *Polymers* **2023**, *15*, 85. <https://doi.org/10.3390/polym15010085>

Academic Editors: Raluca Nicoleta Darie-Niță and Maria Răpă

Received: 8 November 2022

Revised: 17 December 2022

Accepted: 22 December 2022

Published: 25 December 2022



Copyright: © 2022 by the authors. Licensee MDPI, Basel, Switzerland. This article is an open access article distributed under the terms and conditions of the Creative Commons Attribution (CC BY) license (<https://creativecommons.org/licenses/by/4.0/>).

1. Introduction

So far, the production and application of traditional petroleum-based plastics have caused severe environmental issues [1]. For instance, according to the 2021 IPCC Sixth Assessment Report (AR6), human activities, such as the massive extraction and abuse of oil, have led to a global temperature rising of about 1.09 °C since the industrial revolution. As a result, human-induced climate change has caused widespread adverse impacts far more than natural climate variability has [2]. These problems clearly indicate that the replacement of petro-based polyesters is extremely necessary [3–6]. It should be emphasized that poly(ethylene terephthalate) (PET) is one of the most used petro-based plastics at present.

The biomass-derived monomer 2,5-furandicarboxylic acid (FDCA) has obtained remarkable interests from both industries and academies in recent years [7,8]. Moreover, due to its similar chemical structure to that of terephthalic acid (TPA), poly(alkylene 2,5-furandicarboxylate)s (PAFs) are also considered as perfect biobased alternatives to PET and its homologues [9–12]. Poly(ethylene 2,5-furandicarboxylate) (PEF) is the one of the most promising polyesters among PAFs [13–17]. PEF has a high glass transition temperature (T_g) of about 77 °C and a high melting temperature (T_m) of around 214 °C, indicating that PEF shows excellent thermal properties [13]. Furthermore, PEF displays outstanding gas barrier properties, which is 11 times in O₂ and 19 times in CO₂ compared to those of PET [14,15]. However, both the poor toughness and the slow crystallization rate of

PEF have seriously restricted its practical applications [13,16–18]. Poly(propylene 2,5-furandicarboxylate) (PPF) [19–21] and poly(butylene 2,5-furandicarboxylate) (PBF) [22–24] were the other two typical PAFs, both of which have been reported thoroughly. PPF shows a slow crystallization rate [19], while PBF shows a relatively fast crystallization rate [23].

Poly(hexamethylene 2,5-furandicarboxylate) (PHF) is one of the homologues of PEF [16,25–27]. Compared to that of PEF (4.2%), PHF shows a high elongation at break (ϵ_b) of 210%, while it still possesses excellent thermal properties and strong crystallizability [16]. Papageorgiou et al. reported that PHF showed a T_g of 7 °C, a T_m of 145 °C, and an equilibrium melting temperature (T_m°) of 157 °C [25]. PHF exhibited multiple melting behavior due to the melting, recrystallization, and remelting after isothermal crystallization. The gas barrier properties of PHF were slightly reduced compared to those of PEF, but were still better than those of PET [27].

Sebacic acid (SeA), a long-chain fatty acid extracted from castor oil, is a widely available and inexpensive biobased monomer. In a previous study, we synthesized and investigated the isothermal and nonisothermal crystallization kinetics of poly(ethylene succinate-*co*-sebacate) (PESSe) copolyesters [28]. Increasing the ethylene sebacate (ESe) content reduced both the crystallization rate parameter and the crystallization rate coefficient of PESSe copolyesters, suggesting that PESSe copolyesters with higher ESe content crystallized more slowly than those with lower ESe content. [28]. SeA is also often used as a third monomer to manipulate the mechanical property of polyesters [18,29]. In previous research, we prepared poly(butylene succinate)-*b*-poly (butylene sebacate) (PBS-*b*-PBSe) multiblock copolyesters. When the weight content of PBSe was about 40%, the ϵ_b increased significantly from 51.7% for PBS to 673.6% for PBS-*b*-PBSe [29]. Zhou et al. also prepared a series of poly(glycol furandicarboxylate-*co*-glycol sebacate) (PESF) copolyesters through introducing sebacic acid as a third monomer into PEF, which remarkably reduced the crystallinity and improved the ϵ_b of PEF [18].

Copolymerization is an easy way to regulate the thermal and mechanical properties of polymers [22,30–35]. A small amount of research on the copolymerization modification of PHF has been reported in the literature [8,36–38]. For instance, Kasmi et al. synthesized highly heat-resistant poly(hexamethylene-*co*-isosorbide-2,5-furandicarboxylates) copolyesters (PHIsF) [8]. The T_g values gradually increased from 10 to 135 °C with the addition of the third monomer, which enhanced the thermal properties of PHF. In a previous study, we synthesized poly(hexamethylene 2,5-furandicarboxylate-*co*-adipate) copolyesters (PHFA) [37]. Upon increasing the hexamethylene adipate (HA) unit content, the T_m , T_m° , and crystallinity of PHFA gradually decreased; however, on the contrary, the ϵ_b remarkably increased to 498.3% for PHFA30 (HA mol% = 30 mol%) from 197.3% for PHF [38].

To the best of our knowledge, the synthesis and properties of fully biobased poly(hexamethylene 2,5-furandicarboxylate-*co*-sebacate) (PHFSe) copolyesters have not been reported in detail in the literature so far. In this research, we first synthesized PHFSe copolyesters using 1,6-hexanediol (HDO), SeA, and dimethyl 2,5-furandicarboxylate (DMFD) as the monomers; furthermore, we extensively investigated the thermal and mechanical properties of PHFSe copolyesters and compared them with those of PHF to clarify the influence of low contents of hexamethylene sebacate (HSe) unit. It is expected that the results reported herein should be interesting and important for a better understanding of the structure and property relationship of biobased polyesters from a sustainable viewpoint.

2. Experimental

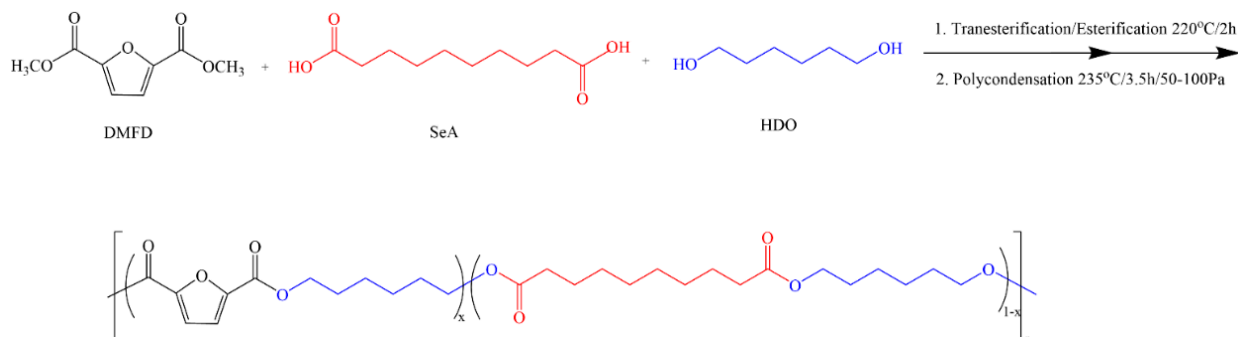
2.1. Materials

The materials' information, including the monomers (HDO, SeA, and DMFD) and the catalyst tetrabutyl titanate (TBT), is shown in the Supporting Information for brevity.

2.2. Synthesis of PHFSe Copolyesters

PHFSe copolyesters were synthesized from DMFD, SeA, and HDO by a two-step melt polycondensation method [25,37]. The detailed synthesis procedure is also described

in the Supporting Information for simplicity. Scheme 1 briefly describes the synthesis route. The copolyesters were abbreviated as PHFSe10, PHFSe20, and PHFSe30, with the number indicating the molar composition of the HSe unit. For comparison, PHF was also synthesized through a similar method.



Scheme 1. Synthesis route of PHFSe copolyesters.

2.3. Characterizations

The chemical structure, composition, thermal stability, basic thermal behavior, melt crystallization behavior, isothermal crystallization kinetics, crystal structure, and tensile mechanical property of PHFSe copolyesters were extensively studied with various techniques and compared with those of PHF. The detailed instruments and experimental conditions were similar to those described elsewhere in a previous study [37]. For brevity, they are also described in the Supporting Information.

3. Results and Discussion

3.1. Composition and $[\eta]$ Values of PHF and PHFSe Copolyesters

The chemical structure and composition of PHF and PHFSe copolyesters were first determined with ^1H NMR. Figure 1 depicts the related ^1H NMR spectra. As shown in Figure 1, for the PHF homopolyester, the signal at 7.19 ppm was from the proton *a* of the furan ring, while the signals at 4.33 ppm, 1.78 ppm, and 1.48 ppm were from the protons *b*₁, *c*₁, and *d*₁, respectively, of the hexamethylene 2,5-furandicarboxylate unit. In addition, for PHFSe copolyesters, the signals at 4.06 ppm (from the proton *b*₂) and 1.60 ppm (from the protons *c*₂ and *d*₂) were from HDO in the HSe unit, while the signals at 2.28 ppm (from the proton *e*), 1.38 ppm (from the proton *f*), and 1.30 ppm (from the protons *g* and *h*) were from SeA in the HSe unit. The composition of PHFSe copolyesters was acquired by the integral ratio of *a* from DMFD and *e* from SeA. The compositions of the HSe unit in the as-synthesized copolyesters were calculated to be 10, 19, and 29 mol%, respectively. Since the molar ratios of HF/HSe were almost the same as those of DMFD/SeA, PHFSe copolyesters were successfully prepared. For convenience, the three copolymers were abbreviated as PHFSe10, PHFSe20, and PHFSe30, respectively, in terms of the feed molar ratio. The $[\eta]$ of PHF and PHFSe copolyesters was calculated using the Solomon–Ciuta equation [39], and the $[\eta]$ values of PHF, PHFSe10, PHFSe20, and PHFSe30 were 0.63, 0.68, 0.62, and 0.63 dL/g, respectively. The similar $[\eta]$ values indicate that PHF and PHFSe copolyesters showed relatively high and similar molecular weights. The above data are recorded in Table 1.

3.2. Thermal Properties and Crystal Structure Studies

The thermal stability of polymeric materials is an important factor from polymer processing and practical application viewpoints. Figure 2 shows both the TGA curves and the derivative thermogravimetry (DTG) curves of PHF and PHFSe copolyesters at a heating rate of 20 °C/min under nitrogen atmosphere. The thermal decomposition temperature at weight loss of 5% (*T*_d) values of all samples were close to or even above 375 °C, indicating that both PHF and PHFSe showed the good thermal stability. From Figure 2, all polyesters

displayed the similar one-step thermal degradation process. As the HSe units content increased, the T_d values of copolyesters slightly increased; moreover, the temperature at maximum degradation rate (T_{max}) shifted slightly to a higher temperature range. The related data are summarized in Table 2 for comparison.

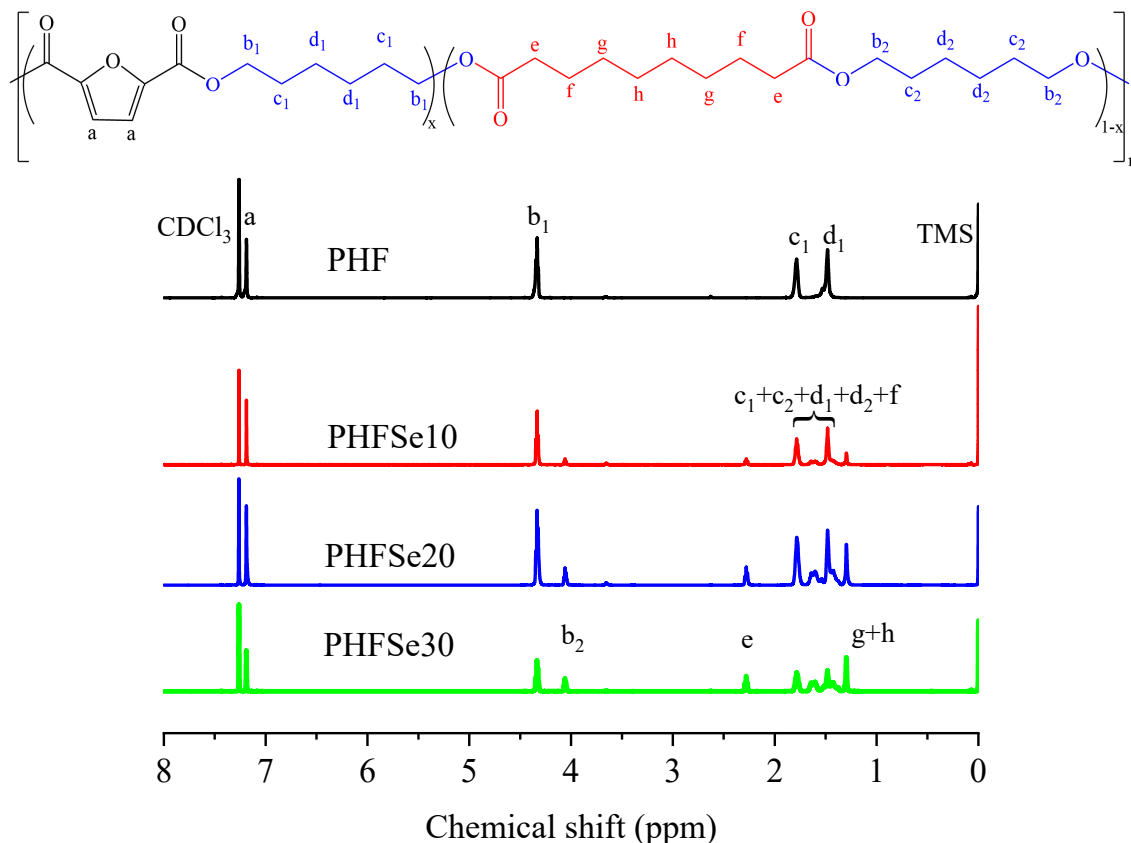


Figure 1. Chemical structure and ^1H NMR spectra of PHF and PHFSe copolyesters.

Table 1. Compositions and $[\eta]$ of PHF and PHFSe copolyesters.

Samples	DMFD/SeA in Feed (mol%)	HF/HSe in Copolyesters (mol%)	$[\eta]$ (dL/g)
PHF	100/0	100/0	0.63
PHFSe10	90/10	90/10	0.68
PHFSe20	80/20	81/19	0.62
PHFSe30	70/30	71/29	0.63

Table 2. Basic thermal behavior data of PHF and PHFSe copolyesters.

Samples	T_d ($^{\circ}\text{C}$)	T_{max} ($^{\circ}\text{C}$)	T_g ($^{\circ}\text{C}$)	T_{ch} ($^{\circ}\text{C}$)	ΔH_{ch} (J/g)	T_m ($^{\circ}\text{C}$)	ΔH_m (J/g)	T_{cc} ($^{\circ}\text{C}$)	ΔH_{cc} (J/g)	T_m° ($^{\circ}\text{C}$)
PHF	374.6	393.6	12.3	55.4	12.3	147.4	48.1	97.2	52.6	154.3
PHFSe10	379.4	401.9	-0.9	40.4	4.5	136.8	42.7	89.2	47.2	148.6
PHFSe20	379.8	403.3	-8.4	33.1	23.6	126.0	41.2	69.2	42.0	144.5
PHFSe30	385.1	408.1	-21.0	22.3	22.5	111.2	35.3	51.8	36.5	142.3

In this section, the basic thermal behavior of PHF and PHFSe copolyesters was studied with DSC. Figure 3 shows the DSC traces of PHF and PHFSe copolyesters at a heating rate of $20\text{ }^{\circ}\text{C}/\text{min}$ after a melt-quenching process. The T_g of PHF was $12.3\text{ }^{\circ}\text{C}$, while

the T_g of PHFSe copolyesters obviously shifted downward to a low temperature range with increasing the HSe unit content due to the increased the chain mobility. Both PHF and PHFSe polyesters showed the cold crystallization and subsequent melting behavior during the second heating process. The cold crystallization temperature (T_{ch}) of PHF was 55.4 °C, while it gradually changed to 40.4 °C, 33.1 °C, and 22.3 °C for PHFSe10, PHFSe20, and PHFSe30, respectively. The cold crystallization enthalpy (ΔH_{ch}) values were also measured. In addition, the T_m of PHFSe30 significantly decreased to 111.2 °C; furthermore, the melting enthalpy (ΔH_m) decreased from 48.1 J/g for PHF to 35.3 J/g for PHFSe30 due to the copolymerization. As a result, the thermal properties of PHF may be obviously influenced and easily adjusted through copolymerization with SeA as the third comonomer in this research.

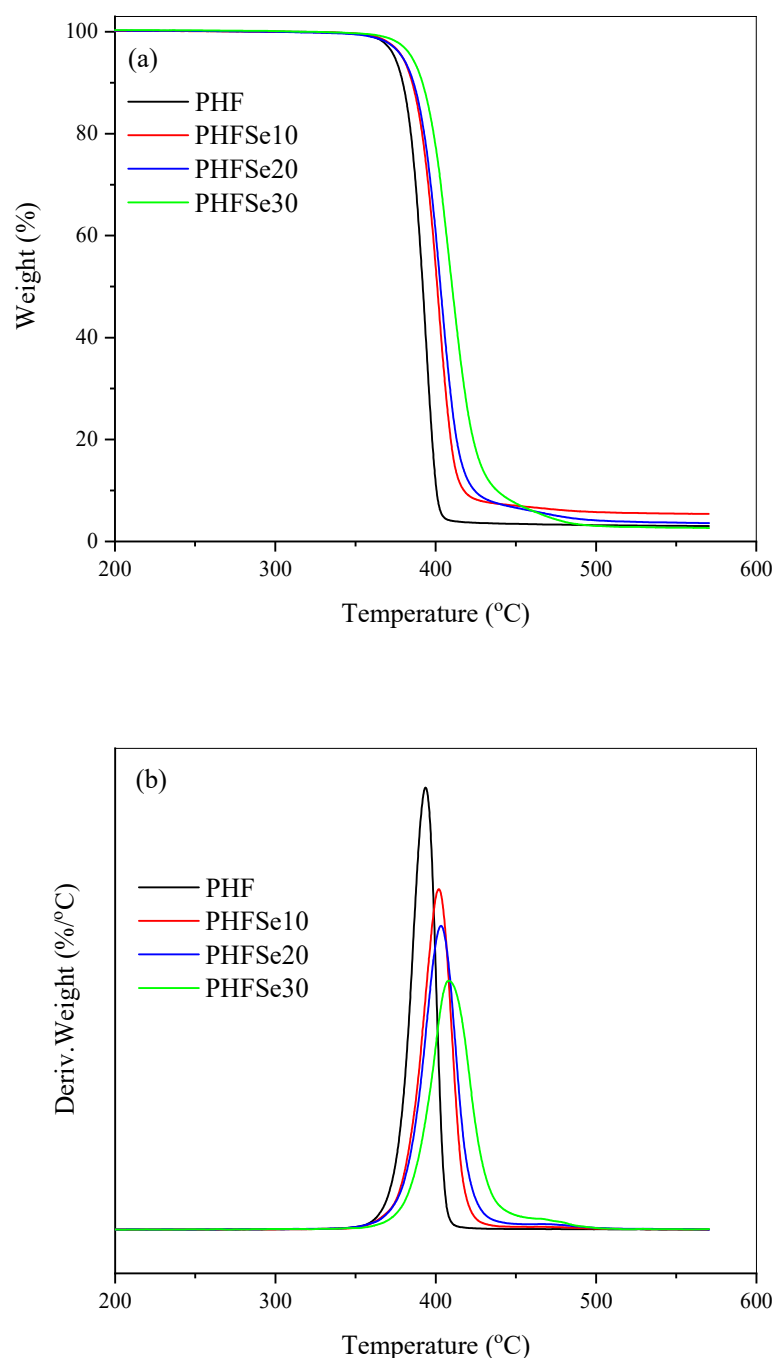


Figure 2. Thermal stability study of PHF and PHFSe copolyesters: (a) TGA and (b) DTG curves.

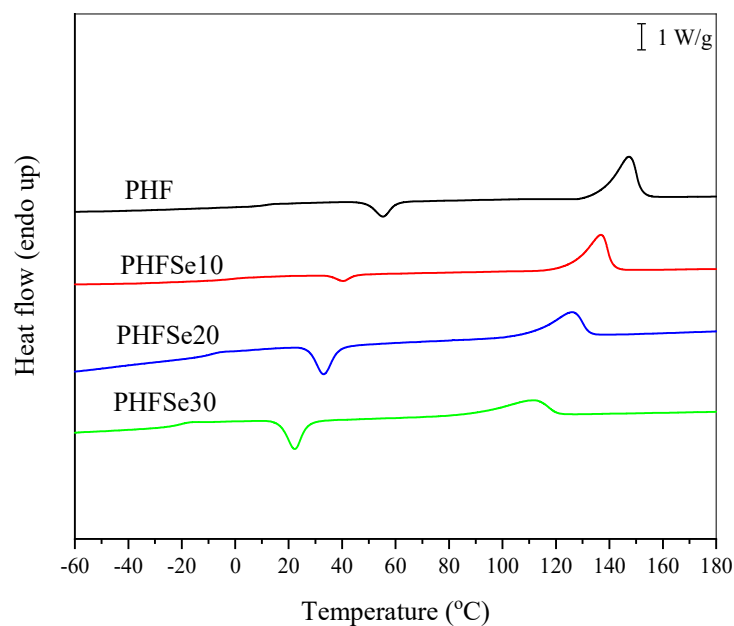


Figure 3. DSC heating curves of PHF and PHFSe copolyesters at 20 °C/min after quenching from molten state.

DSC was also used to study the melt crystallization behavior of PHF and PHFSe copolyesters at a cooling rate of 10 °C/min. The relevant crystallization exotherms are illustrated in Figure 4. In the case of PHF, the melt crystallization temperature (T_{cc}) and melt crystallization enthalpy (ΔH_{cc}) were 97.2 °C and 52.6 J/g, respectively. In the case of PHFSe copolyesters, as the HSe units content increased, the T_{cc} apparently shifted downward to a lower temperature range; moreover, the ΔH_{cc} gradually decreased. For instance, the T_{cc} and ΔH_{cc} of PHFSe30 remarkably decreased to 51.8 °C and 36.5 J/g, respectively. The above results revealed that copolymerization with SeA greatly suppressed the crystallizability of PHF.

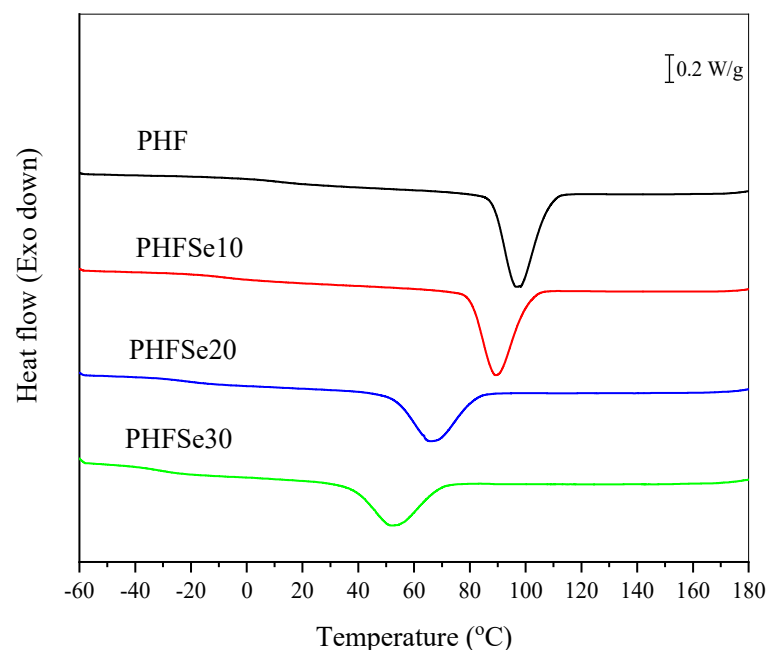


Figure 4. DSC cooling curves at 10 °C/min of PHF and PHFSe copolyesters.

The isothermal melt crystallization kinetics of PHF and PHFSe copolyesters were further investigated with DSC. The plots of relative crystallinity versus time are displayed in Figure 5 for PHF and PHFSe copolyesters. As the degree of supercooling decreased, the crystallization time of all samples became obviously longer with an increase in crystallization temperature (T_c).

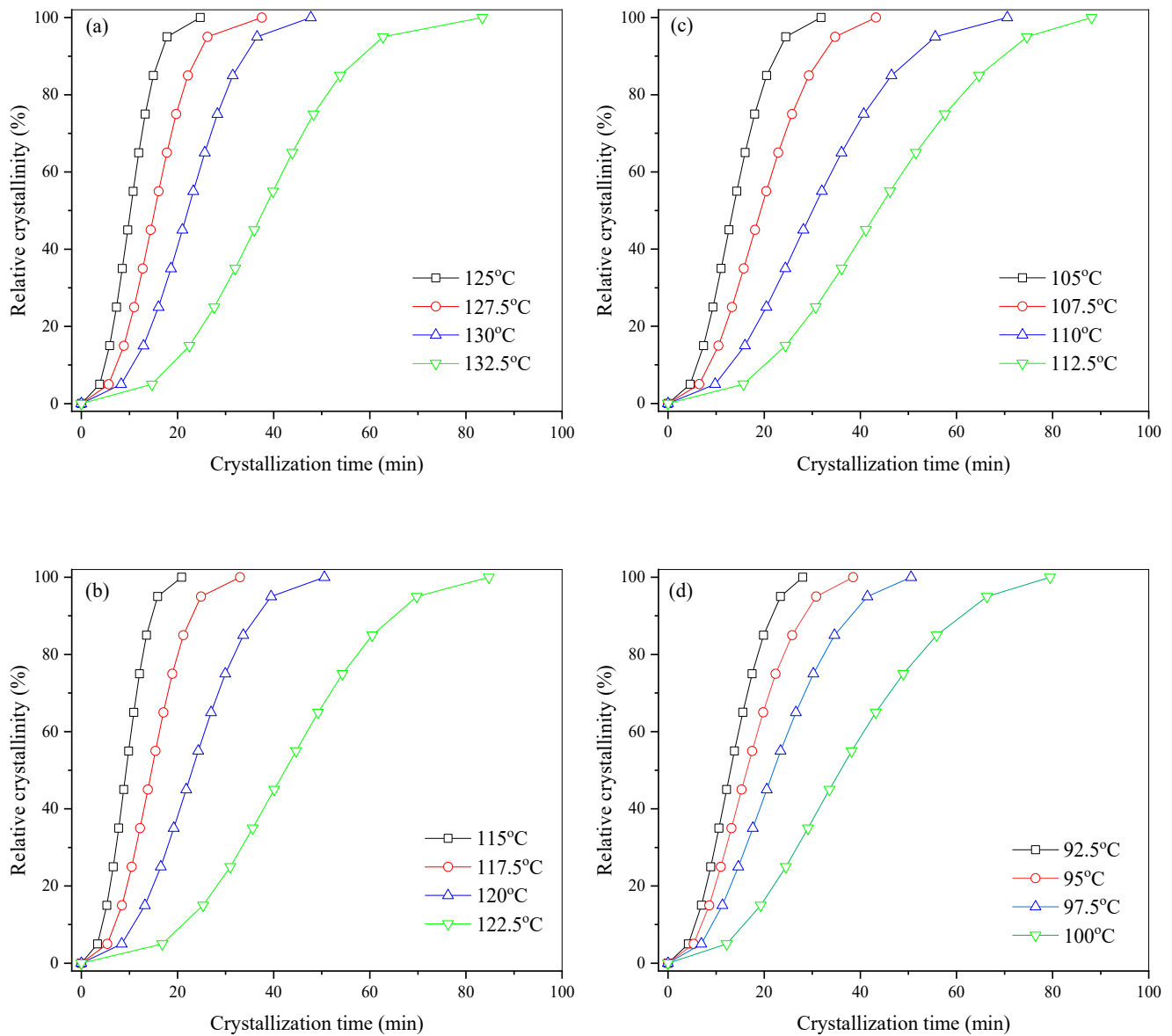


Figure 5. Plots of relative crystallinity versus crystallization time for (a) PHF, (b) PHFSe10, (c) PHFSe20, and (d) PHFSe30.

The isothermal melt crystallization kinetics were studied by the Avrami equation. The relationship between relative crystallinity (X_t) and crystallization time (t) may be described as follows:

$$1 - X_t = \exp(-kt^n) \quad (1)$$

where n is the Avrami exponent, and k is the crystallization rate constant related to both nucleation process and crystal growth [40,41]. The Avrami plots are displayed in Figure 6. The almost-parallel straight lines indicated that the Avrami method fitted the isothermal melt crystallization process of all the samples very well.

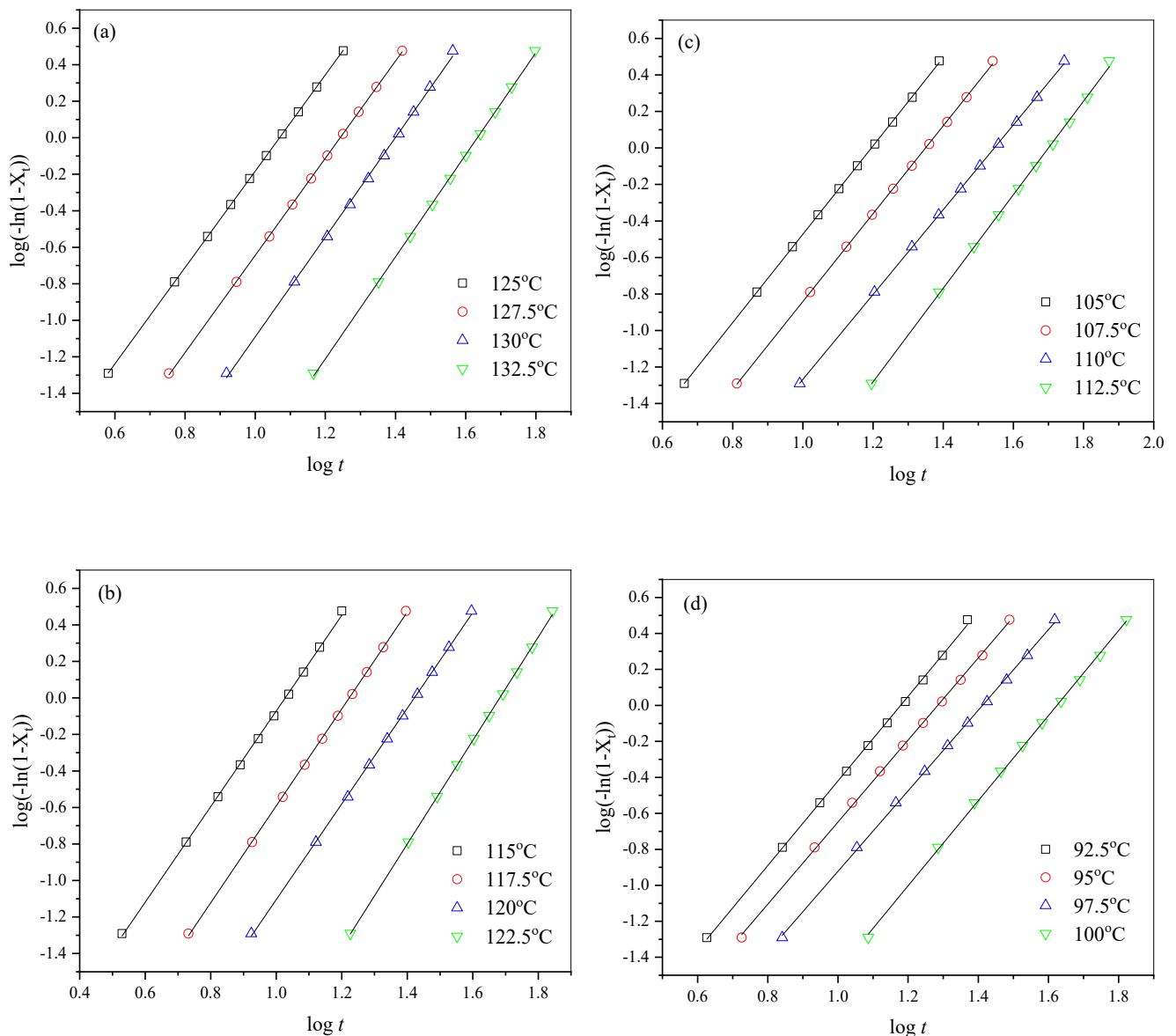


Figure 6. The related Avrami plots for (a) PHF, (b) PHFSe10, (c) PHFSe20, and (d) PHFSe30.

From Figure 6, the values of n and k were acquired and are listed in Table 3. The n values slightly varied between 2.2 and 2.8, suggesting that the crystallization mechanism remained unchanged. The k values gradually decreased with the increase in T_c , suggesting a slower crystallization rate. For a better comparison, crystallization half-time ($t_{0.5}$) was calculated through the following equation:

$$t_{0.5} = \left(\frac{\ln 2}{k}\right)^{\frac{1}{n}} \quad (2)$$

The calculated $t_{0.5}$ data are also shown in Table 3. For each sample, $t_{0.5}$ gradually increased with the increase in T_c , indicating that the increase in T_c decreased the crystallization rate.

The subsequent melting behavior was also studied with DSC for PHF and PHFSe copolyesters after they finished the isothermal melt crystallization at the indicated T_c s. Figure S1 in the Supporting Information demonstrates the relevant melting behavior. Both PHF and PHFSe copolyesters displayed a single melting endotherm at each T_c , which gradually increased with T_c .

Table 3. Summary of the Avrami parameters for PHF and PHFSe copolyesters.

Samples	T_c (°C)	n	k (min ⁻ⁿ)	$t_{0.5}$ (min)
PHF	125.0	2.6	1.50×10^{-3}	10.21
	127.5	2.7	4.93×10^{-4}	15.21
	130.0	2.7	1.50×10^{-4}	21.93
	132.5	2.8	2.72×10^{-5}	37.68
PHFSe10	115.0	2.6	2.04×10^{-3}	9.26
	117.5	2.7	5.69×10^{-4}	14.54
	120.0	2.6	1.88×10^{-4}	22.95
PHFSe20	122.5	2.8	1.70×10^{-5}	42.27
	105.0	2.4	1.28×10^{-3}	13.48
	107.5	2.4	5.66×10^{-4}	19.21
	110.0	2.3	2.56×10^{-4}	30.00
PHFSe30	112.5	2.6	4.39×10^{-5}	43.42
	92.5	2.4	1.69×10^{-3}	12.91
	95.0	2.3	1.17×10^{-3}	16.39
	97.5	2.2	6.88×10^{-4}	21.92
	100.0	2.4	1.45×10^{-4}	36.02

The T_m° values of PHF and PHFSe copolymers were further derived through the classic Hoffman–Weeks equation as follows [42]:

$$T_m = (1 - \eta)T_m^\circ + \eta T_c \tag{3}$$

where T_m represents the apparent melting temperature at T_c , and η assumes values between 0 and 1 and is regarded as a measure of the stability, i.e., the lamellar thickness of the crystals undergoing the melting process. Figure 7 demonstrates the Hoffman–Weeks plots for PHF and PHFSe copolyesters. The T_m° values were thus derived to be 154.3, 148.6, 144.5, and 142.3 °C for PHF, PHFSe10, PHFSe20, and PHFSe30, respectively. In brief, with the increase in HSe unit content, the T_m° values accordingly decreased.

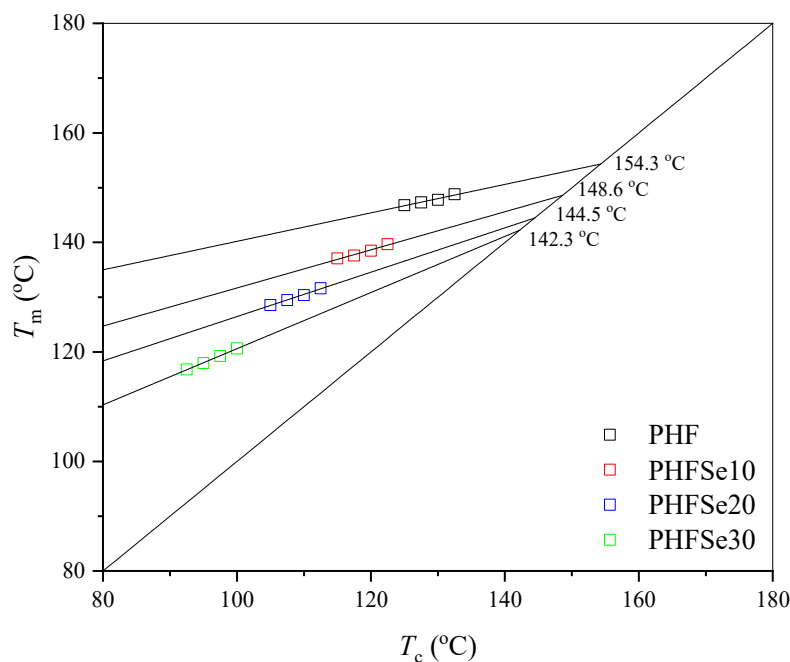


Figure 7. Hoffman–Weeks plots of PHF and PHFSe copolyesters.

The influence of HSe unit on the crystal structure of PHF was studied by wide-angle X-ray diffraction (WAXD). Figure 8 illustrates the WAXD profiles. PHF showed three

characteristic diffraction peaks at $2\theta = 13.6^\circ$, 17.0° , and 24.7° , respectively. In the case of PHFSe copolyesters, they displayed similar WAXD profiles to PHF, suggesting that the presence of HSe unit did not modify the crystal structure of PHF. At present, it is not certain whether the HSe units are totally excluded from the PHF crystals or are partly included into the PHF crystals. Further investigation is necessary to address this issue and will be reported in forthcoming research. In addition, the crystallinity (X_c) of each sample was estimated from Figure 8. The X_c values of PHF, PHFSe10, PHFSe20, and PHFSe30 were about 43%, 33%, 23%, and 20%, respectively, revealing again that the copolymerization with SeA reduced the crystallinity of PHF.

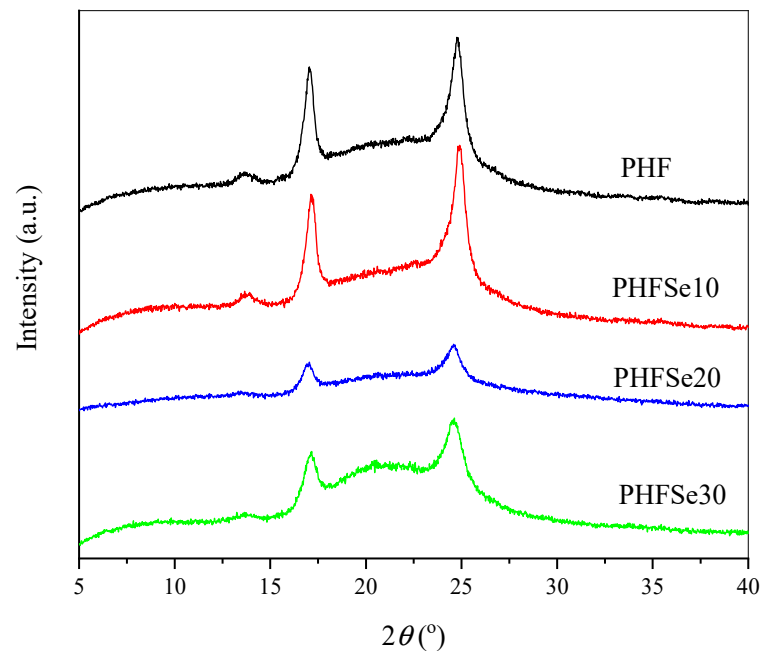


Figure 8. WAXD patterns of PHF and PHFSe copolyesters.

3.3. Tensile Mechanical Property Study

The influence of low contents of HSe unit on the tensile mechanical property of PHF-based copolyesters was further studied in this section. The stress–strain curves of PHF and PHFSe copolyesters are shown in Figure 9. The increase in HSe unit from 0 to 30 mol% decreased the yield strength (σ_y) from 24.2 ± 0.6 to 8.1 ± 0.2 MPa, the tensile strength (σ_b) from 30.3 ± 1.4 to 17.3 ± 1.4 MPa, and the Young's modulus (E_t) from 565.6 ± 23.1 to 114.9 ± 1.5 MPa, respectively. On the contrary, the ε_b increased from $261.6 \pm 8.3\%$ for PHF to $513.2 \pm 33.8\%$ for PHFSe30, suggesting a remarkably improved toughness. The mechanical property data are summarized in Table 4.

Table 4. Summary of the mechanical property of PHF and PHFDGA copolyesters.

Samples	E_t (MPa)	σ_y (MPa)	ε_y (%)	σ_b (MPa)	ε_b (%)
PHF	565.6 ± 23.1	24.2 ± 0.6	16.2 ± 1.2	30.3 ± 1.4	261.6 ± 8.3
PHFSe10	320.0 ± 10.3	19.1 ± 0.8	21.9 ± 0.3	24.4 ± 0.4	274.6 ± 18.5
PHFSe20	205.7 ± 8.5	13.7 ± 0.2	23.0 ± 1.4	23.6 ± 2.4	435.8 ± 18.2
PHFSe30	114.9 ± 1.5	8.1 ± 0.2	22.3 ± 1.9	17.3 ± 1.4	513.2 ± 33.8

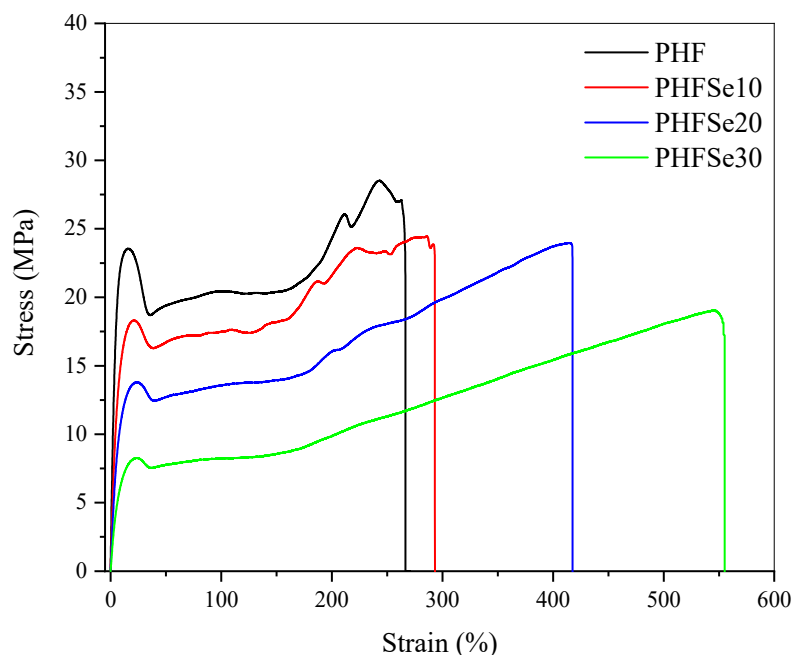


Figure 9. Stress–strain curves of PHF and PHFSe copolyesters.

4. Conclusions

In this research, three novel, fully biobased PHFSe copolyesters containing low contents of HSe unit from 10 to 30 mol% were successfully synthesized through a common melt polycondensation method from all the biobased monomers, as evidenced by the ^1H NMR results. Both PHFSe copolyesters and PHF had relatively high and similar intrinsic viscosity values of 0.62 dL/g and above. The thermal behavior (including thermal stability, basic thermal parameters, and crystallization behavior) and mechanical property of PHFSe copolyesters were systematically reported and compared with those of the PHF homopolymer. Regardless of the HSe unit content, both PHFSe copolyesters and PHF showed the high thermal stability. The glass transition temperature, melting temperature, and equilibrium melting temperature gradually decreased by increasing the HSe unit content due to the presence of the flexible HSe segment with a high chain mobility. The copolymerization with SeA reduced the crystallizability of PHF. For instance, the melt crystallization temperature decreased from 97.2 °C for PHF to 51.8 °C for PHFSe30 during a cooling process from the melt at 10 °C/min. The isothermal melt crystallization kinetics study indicated that all samples crystallized more slowly, with an increasing crystallization temperature due to the decrease in the degree of supercooling. The presence of HSe unit did not change the crystal structure of PHF. The tensile mechanical property was further studied, which obviously varied with the HSe unit content. For instance, the elongation at break obviously increased from $261.6 \pm 8.3\%$ for PHF to $513.2 \pm 33.8\%$ for PHFSe30. In brief, the thermal and mechanical properties of PHF-based copolyesters may be easily tuned by controlling the HSe unit content in this contribution to meet various practical end-use requirements.

Supplementary Materials: The following supporting information can be downloaded at: <https://www.mdpi.com/article/10.3390/polym15010085/s1>, Figure S1: Melting behavior of (a) PHF, (b) PHFSe10, (c) PHFSe20, and (d) PHFSe30 after isothermal crystallization at indicated T_{cs} .

Author Contributions: S.F.; investigation; writing—original draft preparation; Z.J.; supervision; Z.Q.; supervision; writing—review and editing; funding acquisition. All authors have read and agreed to the published version of the manuscript.

Funding: National Natural Science Foundation, China (51573016, 51521062 and 52173019).

Institutional Review Board Statement: Not applicable.

Data Availability Statement: The data presented in this study are available on request from the corresponding author.

Acknowledgments: Thanks are due to the National Natural Science Foundation, China (51573016, 51521062, and 52173019) for the financial support of this research.

Conflicts of Interest: The authors declare no conflict of interest.

References

1. Bilo, F.; Pandini, S.; Sartore, L.; Depero, L.; Gargiulo, G.; Bonassi, A.; Federici, S.; Bontempi, E. A sustainable bioplastic obtained from rice straw. *J. Clean. Prod.* **2018**, *200*, 357–368. [[CrossRef](#)]
2. Su, B.; Chen, Z.; Huang, J. Impact attribution of climate change: The new cognition from IPCC AR6 WGII. *J. Trans. Atmos. Sci.* **2022**, *45*, 512–519.
3. Sheldon, R. Utilisation of biomass for sustainable fuels and chemicals: Molecules, methods and metrics. *Catal. Today* **2011**, *167*, 3–13. [[CrossRef](#)]
4. Gallezot, P. ChemInform abstract: Conversion of biomass to selected chemical products. *Chem. Soc. Rev.* **2012**, *41*, 1538–1558. [[CrossRef](#)]
5. Iwata, T. Biodegradable and bio-based polymers: Future prospects of eco-friendly plastics. *Angew. Chem. Int. Ed.* **2015**, *54*, 3210–3215. [[CrossRef](#)]
6. Bond, J.; Alonso, D.; Wang, D.; West, R.; Dumesic, J. Integrated catalytic conversion of gamma-valerolactone to liquid alkenes for transportation fuels. *Science* **2010**, *327*, 1110–1114. [[CrossRef](#)] [[PubMed](#)]
7. Motagamwala, A.; Won, W.; Sener, C.; Alonso, D.; Maravelias, C.; Dumesic, J. Toward biomass-derived renewable plastics: Production of 2,5-furandicarboxylic acid from fructose. *Sci. Adv.* **2018**, *4*, 9722. [[CrossRef](#)] [[PubMed](#)]
8. Kasmi, N.; Ainali, N.; Agapiou, E.; Papadopoulos, L.; Papageorgiou, G.; Bikiaris, D. Novel high Tg fully biobased poly(hexamethylene-co-isosorbide-2,5-furan dicarboxylate) copolyesters: Synergistic effect of isosorbide insertion on thermal performance enhancement. *Polym. Degrad. Stab.* **2019**, *169*, 108983. [[CrossRef](#)]
9. Wu, J.; Xie, H.; Wu, L.; Li, B.; Dubois, P. Correction: DBU-catalyzed biobased poly(ethylene 2,5-furandicarboxylate) polyester with rapid melt crystallization: Synthesis, crystallization kinetics and melting behavior. *RSC Adv.* **2017**, *7*, 13877. [[CrossRef](#)]
10. Lotti, N.; Munari, A.; Gigli, M.; Gazzano, M.; Tsanaktsis, V.; Bikiaris, D.; Papageorgiou, G. Thermal and structural response of in situ prepared biobased poly(ethylene 2,5-furandicarboxylate) nanocomposites. *Polymer* **2016**, *103*, 288–298. [[CrossRef](#)]
11. Van Berkel, J.; Guigo, N.; Kolstad, J.; Sipos, L.; Wang, B.; Dam, M.; Sbirrazzuoli, N. Isothermal crystallization kinetics of poly(ethylene 2,5-furandicarboxylate). *Macromol. Mater. Eng.* **2015**, *300*, 466–474. [[CrossRef](#)]
12. Codou, A.; Guigo, N.; Van Berkel, J.; De Jong, E.; Sbirrazzuoli, N. Non-isothermal crystallization kinetics of biobased poly(ethylene 2,5-furandicarboxylate) synthesized via the direct esterification process. *Macromol. Chem. Phys.* **2015**, *215*, 2065–2074. [[CrossRef](#)]
13. Knoop, R.; Vogelzang, W.; Haveren, J.; Es, D. High molecular weight poly(ethylene-2,5-furanoate); Critical aspects in synthesis and mechanical property determination. *J. Polym. Sci. Polym. Chem.* **2013**, *51*, 4191–4199. [[CrossRef](#)]
14. Burgess, S.; Karvan, O.; Johnson, J.; Kriegel, R.; Koros, W. Oxygen sorption and transport in amorphous poly(ethylene furanoate). *Polymer* **2014**, *55*, 4748–4756. [[CrossRef](#)]
15. Burgess, S.; Kriegel, R.; Koros, W. Carbon dioxide sorption and transport in amorphous poly(ethylene furanoate). *Macromolecules* **2015**, *48*, 2184–2193. [[CrossRef](#)]
16. Jiang, M.; Liu, Q.; Zhang, Q.; Ye, C.; Zhou, G. A series of furan-aromatic polyesters synthesized via direct esterification method based on renewable resources. *J. Polym. Sci. Polym. Chem.* **2012**, *50*, 1026–1036. [[CrossRef](#)]
17. Wang, J.; Liu, X.; Zhang, Y.; Liu, F.; Zhu, J. Modification of poly(ethylene 2,5-furandicarboxylate) with 1,4-cyclohexanedimethylene: Influence of composition on mechanical and barrier properties. *Polymer* **2016**, *103*, 1–8. [[CrossRef](#)]
18. Wang, G.; Jiang, M.; Zhang, Q.; Wang, R.; Zhou, G. Biobased copolyesters: Synthesis, crystallization behavior, thermal and mechanical properties of poly(ethylene glycol sebacate-co-ethylene glycol 2,5-furan dicarboxylate). *RSC Adv.* **2017**, *7*, 13798–13807. [[CrossRef](#)]
19. Wang, K.; Zhang, K.; Jiang, Z.; Qiu, Z. Biobased poly(1,3-propylene 2,5-furandicarboxylate)-carbon nanotubes nanocomposites with enhanced thermal, mechanical properties and crystallization behavior. *J. Polym. Environ.* **2022**, *30*, 555–561. [[CrossRef](#)]
20. Parageogios, G.; Papageorgiou, D.; Tsanaktsis, V.; Bikiaris, D. Synthesis of the bio-based polyester poly(propylene 2,5-furan dicarboxylate). comparison of thermal behavior and solid state structure with its terephthalate and naphthalate homologues. *Polymer* **2015**, *62*, 28–38.
21. Righetti, M.; Marchese, P.; Vannini, M.; Celli, A.; Lorenzetti, C.; Cavallo, D. Polymorphism and multiple melting behavior of bio-based poly(propylene 2,5-furandicarboxylate). *Biomacromolecules* **2020**, *21*, 2622–2634. [[CrossRef](#)] [[PubMed](#)]
22. Wu, B.; Xu, Y.; Bu, Z.; Wu, L.; Li, B.; Dubois, P. Biobased poly(butylene 2,5-furandicarboxylate) and poly(butylene adipate-co-butylene 2,5-furandicarboxylate)s: From synthesis using highly purified 2,5-furandicarboxylic acid to thermo-mechanical properties. *Polymer* **2014**, *55*, 3648–3655. [[CrossRef](#)]
23. Pouloupoulou, N.; Nikolaidis, G.; Ioannidis, R.; Efstathiadou, V.; Terzopoulou, Z.; Papageorgiou, D.; Kapnisti, M.; Papageorgiou, G. Aromatic but sustainable: Poly(butylene 2,5-furandicarboxylate) as a crystallizing thermoplastic in the bioeconomy. *Ind. Eng. Chem. Res.* **2022**, *61*, 13461–13473. [[CrossRef](#)]

24. Bi, T.; Qiu, Z. Synthesis thermal and mechanical properties of fully biobased poly(butylene-co-propylene 2,5-furandicarboxylate) copolyesters with low contents of propylene 2,5-furandicarboxylate units. *Polymer* **2020**, *186*, 122053. [[CrossRef](#)]
25. Papageorgiou, G.; Tsanaktsis, V.; Papageorgiou, D.; Chrissafis, K.; Exarhopoulos, S.; Bikiaris, D. Furan-based polyesters from renewable resources: Crystallization and thermal degradation behavior of poly(hexamethylene 2,5-furan-dicarboxylate). *Eur. Polym. J.* **2015**, *67*, 383–396. [[CrossRef](#)]
26. Zhang, J.; Liang, Q.; Xie, W.; Peng, L.; He, L.; He, Z. An eco-friendly method to get a bio-based dicarboxylic acid monomer 2,5-furandicarboxylic acid and its application in the synthesis of Poly(hexylene 2,5-furandicarboxylate) (PHF). *Polymers* **2019**, *11*, 197. [[CrossRef](#)] [[PubMed](#)]
27. Guidotti, G.; Soccio, M.; Garcia-Gutierrez, M.C.; Ezquerra, T.; Siracusa, V.; Gutierrez-Fernandez, E. Fully biobased superpolymers of 2,5-furandicarboxylic acid with different functional properties: From rigid to flexible, high performant packaging materials. *ACS Sustain. Chem. Eng.* **2020**, *8*, 9558–9568. [[CrossRef](#)]
28. Qiu, S.; Su, Z.; Qiu, Z. Isothermal and nonisothermal crystallization kinetics of novel biobased poly(ethylene succinate-co-ethylene sebacate) copolymers from the amorphous state. *J. Therm. Anal. Calorim.* **2017**, *129*, 801–808. [[CrossRef](#)]
29. Shang, Y.; Jiang, Z.; Qiu, Z. Synthesis, thermal and mechanical properties of novel biobased, biodegradable and double crystalline poly(butylene succinate)-*b*-Poly (butylene sebacate) multiblock copolymers. *Polymer* **2021**, *214*, 123248. [[CrossRef](#)]
30. Papadopoulos, L.; Magaziotis, A.; Nerantzaki, M.; Terzopoulou, Z.; Papageorgiou, G.; Bikiaris, D. Synthesis and characterization of novel poly(ethylene furanoate-co-adipate) random copolyesters with enhanced biodegradability. *Polym. Degrad. Stab.* **2018**, *156*, 32–42. [[CrossRef](#)]
31. Terzopoulou, Z.; Tsanaktsis, V.; Bikiaris, D.; Exarhopoulos, S.; Papageorgiou, D.; Papageorgiou, G. Biobased poly(ethylene furanoate-co-ethylene succinate) copolyesters: Solid state structure, melting point depression and biodegradability. *RSC Adv.* **2016**, *6*, 84003. [[CrossRef](#)]
32. Wang, G.; Jiang, M.; Zhang, Q.; Wang, R.; Tong, X.; Xue, S.; Zhou, G. Biobased copolyesters: Synthesis, sequence distribution, crystal structure, thermal and mechanical properties of poly(butylene sebacate-co-butylene furandicarboxylate). *Polym. Degrad. Stab.* **2017**, *143*, 1–8. [[CrossRef](#)]
33. Hu, H.; Zhang, R.; Wang, J.; Ying, W.; Zhu, J. Fully bio-based poly(propylene succinate-co-propylene furandicarboxylate) copolyesters with proper mechanical, degradation and barrier properties for green packaging applications. *Eur. Polym. J.* **2018**, *102*, 101–110. [[CrossRef](#)]
34. Hu, H.; Zhang, R.; Jiang, Y.; Shi, L.; Wang, J.; Ying, W.; Zhu, J. Toward biobased, biodegradable, and smart barrier packaging material: Modification of poly(neopentyl glycol 2,5-furandicarboxylate) with succinic acid. *ACS Sustain. Chem. Eng.* **2019**, *7*, 4255–4265. [[CrossRef](#)]
35. Terzopoulou, Z.; Papadopoulos, L.; Zamboulis, A.; Papageorgiou, D.; Papageorgiou, G.; Bikiaris, D. Tuning the properties of furandicarboxylic acid-based polyesters with copolymerization: A review. *Polymers* **2020**, *12*, 1209. [[CrossRef](#)]
36. Little, A.; Pellis, A.; Comerford, J.; Naranjo-Valles, E.; Hafezi, N.; Mascari, M.; Farmer, T. Effects of methyl branching on the properties and performance of furandioate-adipate copolyesters of bio-based secondary diols. *ACS Sustain. Chem. Eng.* **2020**, *8*, 14471–14483. [[CrossRef](#)]
37. Xie, H.; Wu, L.; Li, B.; Dubois, P. Biobased poly(ethylene-co-hexamethylene 2,5- furandicarboxylate) (PEHF) copolyesters with superior tensile properties. *Ind. Eng. Chem. Res.* **2018**, *57*, 13094–13102. [[CrossRef](#)]
38. Chen, M.; Jiang, Z.; Qiu, Z. Synthesis and properties of poly(hexamethylene 2,5-furandicarboxylate-co-adipate) copolyesters. *Eur. Polym. J.* **2021**, *161*, 110860. [[CrossRef](#)]
39. Pamies, R.; Cifre, J.H.; Martínez, M.C.L.; de la Torre, J.G. Determination of intrinsic viscosities of macromolecules and nanoparticles. Comparison of single-point and dilution procedures. *Colloid Polym. Sci.* **2008**, *286*, 1223–1231. [[CrossRef](#)]
40. Avrami, M. Kinetics of phase change. II transformation-time relations for random distribution of nuclei. *J. Chem. Phys.* **1940**, *8*, 212–224. [[CrossRef](#)]
41. Avrami, M. Granulation, phase change, and microstructure kinetics of phase change. III. *J. Chem. Phys.* **1941**, *9*, 177–184. [[CrossRef](#)]
42. Hoffman, J.; Weeks, J. Melting process and the equilibrium melting temperature of polychlorotrifluoroethylene. *J. Res. Natl. Bur. Stand.* **1962**, *66*, 13. [[CrossRef](#)]

Disclaimer/Publisher's Note: The statements, opinions and data contained in all publications are solely those of the individual author(s) and contributor(s) and not of MDPI and/or the editor(s). MDPI and/or the editor(s) disclaim responsibility for any injury to people or property resulting from any ideas, methods, instructions or products referred to in the content.